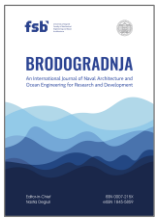
Brodogradnja Volume 78 Number 1 (2027) 78106

University of Zagreb
Faculty of Mechanical
Engineering and Naval
Architecture

journal homepage: www.brodogradnja.fsb.hr

Brodogradnja

An International Journal of Naval Architecture and
Ocean Engineering for Research and Development



Cumulative steel replacement prediction in severely corrosion - affected bulk carriers

Špiro Ivošević[1], *Nataša Kovač*[2], *Nikola Momčilović*[3,*]

[1]*University of Montenegro, Faculty of Maritime Studies Kotor, Put I Bokeljske brigade 44, Kotor, Montenegro*
[2]*University of Donja Gorica, Faculty of Applied Sciences, Oktoih 1, Donja Gorica, Podgorica, Montenegro*
[3]*University of Belgrade, Faculty of Mechanical Engineering, Kraljice Marije 16, Beograd, Serbia*

ARTICLE INFO

Keywords:
Bulk carriers
Steel replacement
Corrosion wastage
Lightship
Ship hull

ABSTRACT

Systematic studies on long-term cumulative steel replacement in ships are virtually absent, despite their importance for ship design, maintenance of ageing vessels, and sustainable shipping. Extensive ultrasonic thickness measurement reports and steel renewal records collected throughout the operational lives of 12 bulk carriers were presented and analysed to quantify cumulative steel replacement at both the ship and their lightweight groups. By combining these data with benchmark shipyard information, the total lightweight mass of the ships is estimated. The findings indicate that cumulative steel replacement may exceed 1000 t over a typical 25-year service life in severely corrosion-affected Handymax bulk carriers. Steel renewal was dominated by the inner bottom and hopper plating, while ships carrying iron, ore and coal generally required substantially greater steel replacement than grain carriers. The main contribution of this work is a complementary predictive framework that combines cell-level machine-learning point estimation with stochastic renewal-based modelling. It provides ship-level and structural-area forecasts, time-dependent replacement schedules, and predictive intervals, and can be applied prospectively to technically specified ships not included in the historical dataset. The proposed methodology provides a practical framework for maintenance planning, structural assessment, ship design, and life-cycle management of ageing vessels.

1. Introduction

During their operational service, which is commonly considered to be around 25 years in the industry, steel ships are subjected to various conditions that impact the hull structure, particularly through corrosion-related aging [1-3]. Corrosion in cargo ships is driven by a combination of factors, including loading and unloading operations, ballast water, exposure to seawater, atmospheric conditions, and other environmental and operational stresses [4]. This phenomenon is directly associated to ship aging [5] and has been repeatedly identified as a contributing factor in structural failures [6-8]. Cargo ships are vulnerable in that context and thus often experience a reduced service life of the hull and its structural elements.

* Corresponding author.
E-mail address: nmomcilovic@mas.bg.ac.rs

https://doi.org/10.21278/brod78106
Received 20 July 2026; Received in revised form 29 September 2026; Accepted 13 October 2026
Available online 03 November 2026
ISSN 0007-215X; eISSN 1845-5859

In the marine environment, various corrosion mechanisms can occur, including general, pitting, intergranular, galvanic, fretting, stress, microbiological, fatigue, crevice, erosion, and cavitation corrosion [9]. Nevertheless, the most significant and evident consequence of corrosion in ships is the reduction of thickness of structural elements [10, 11]. The rate of chemical and mechanical degradation, and thickness diminution, is significantly influenced by corrosion protectives [12]. Consequently, corrosion influences the structural reliability of ship structures, as shown by [13-15].

Most marine corrosion studies focus on test coupons rather than full-scale ship structures. For example, corrosion has been investigated from a chemical perspective by examining the effects of various seawater attributes on the degradation rate of test coupons [16, 17], and from a mechanical perspective in relation to stainless steels used in ship applications [18, 19]. While these studies provide valuable insights into material degradation relevant to shipbuilding, they remain limited to the scale of laboratory specimens.

Beyond studies of local effects, two broader levels are important from the perspective of ship hull structures: the impact of corrosion on single ship structural member and on the ship hull. Regarding the first level, most research have focused on corrosion wastage rates of specific structural members. Examples include studies on the corrosion of fuel tanks [20-22], inner bottom plates [23], ballast tanks [24], and bottom longitudinal members [25, 26].

With respect to the hull structure, research has largely directed towards the effect of corrosion degradation on the ultimate strength of ships. This issue has been particularly examined in bulk carriers [27, 28], and more recently in [29, 30], where corrosion was shown to significantly reduce hull-girder strength. Similar investigations have also been conducted for oil tankers, where methodologies for ultimate strength assessment of corroded ships were developed, see [31]. A more systematic approach to evaluate the effects of corrosion on hull structures has been given in several studies [32, 33].

In terms of rules and regulations, corrosion in ships is addressed in two principal ways. First, during ship design, a corrosion addition is applied either to the calculated net scantlings [34, 35] or incorporated directly within the scantling requirements [36]. The magnitude of this addition depends on the location and function of the structural member. For bulk carriers, these procedures have been consolidated under the IACS Common Structural Rules [37]. Secondly, corrosion is managed during maintenance through periodic surveys [38], where the extent of wastage determines whether plating or structural elements must be renewed. In general, depending on the structural member, steel renewal is required when corrosion wastage exceeds prescribed limits, typically ranging from 10 % to 25 % of the original thickness [34, 35, 39].

Although corrosion wastage rates are well documented in the literature, the cumulative effects of corrosion, and the resulting steel renewals over decades of service, have not been adequately addressed, particularly for series of similar ships such as those examined in this study. Cumulative lifetime corrosion loss directly affects ship design, particularly the lightship mass, which is a critical parameter in ship design process [40, 41]. In addition, recent developments in the evaluation of lightweight mass for various ship types are presented by [42]. It should be noted that the distribution of lightweight mass is also important for longitudinal strength and stability calculations, and any change in this parameter directly influences the allowable deadweight a ship can carry. Moreover, changes in lightship mass directly affect ship efficiency [43-45] and, consequently, compliance with the energy efficiency regulatory framework [46, 47]. Nonetheless, from a regulatory perspective, protective coatings must comply with standards issued by the International Maritime Organization (IMO), see [48, 49]. In addition, steel renewal due to corrosion is also acknowledged by the IMO in the context of ship recycling [50] and is expected to play an increasingly important role in sustainable development [51].

Bulk carriers, which are the focus of this study, represent the backbone of maritime transport, accounting for 43 % of the total deadweight tonnage and 30.7 % of the total number of merchant ships. Their share continues to grow, with deadweight tonnage increasing by 3.1 % between 2023 and 2024, while bulk carriers also represented the largest share of tonnage sold for demolition (40.7 %), see [52]. According to shipping terminology issued by Clarkson, Handymax bulk carriers are defined as ranging from 35000 dwt to 50000 dwt [53], representing a smaller and more flexible segment of the fleet. This definition is adopted in the present paper, although slight variations exist across sources. In light of recent energy efficiency measures that have

slowed the fleet and increased regulatory scrutiny, as shown by [54], the impact of steel renewal and cumulative corrosion on lightship mass becomes particularly relevant, as even marginal reductions in lightship weight can improve ship efficiency, as found for bulk carriers in [55].

To date, and to the best of the authors' knowledge, only one investigation directly comparable in terms of full-scale cumulative steel-replacement data has been conducted, namely the authors' previous study on four Handymax bulk carriers [56]. That work was primarily descriptive within a practical engineering context: it quantified cumulative steel replacement, estimated the masses of lightweight groups, and evaluated corrosion-induced material loss. Owing to the limited sample and considerable data scatter, the resulting relationships were intended mainly for preliminary assessment and did not constitute a predictive framework for ships outside the observed sample. Another relevant study, by [57], showed that reduced corrosion margins for side shell plating, ballast tanks, and hold frames led to substantially higher repair demands after 15 years of service, estimating that a Handymax bulk carrier would require approximately 1440 tons of steel renewal, even under conservative assumptions and with proper maintenance.

Overall, existing research on corrosion in ships, including bulk carriers, focuses on predicting local wastage, studying the chemical and mechanical mechanisms of material degradation, or assessing the influence of corrosion on structural integrity. Systematic quantification of cumulative corrosion loss and steel renewal across a ship's lifetime has received almost no attention. This lack of data is understandable, since long-term measurement records tracking series of ships throughout their entire service lives are rarely collected or accessible. Furthermore, conventional ship weight estimation methods typically provide only a single figure for total hull steel mass, without differentiating between structural regions, leaving the distribution and accumulation of lifetime corrosion losses unexplored.

Therefore, with the support of a certified thickness measurement company (see Acknowledgements), we obtained comprehensive ultrasonic thickness measurement reports and detailed records of steel renewal due to corrosion for 71 Handymax bulk carriers. This study extends the authors' previous work on four bulk carriers, done in [56], providing a significantly broader dataset and assessment. The expanded scope enables more accurate quantification of cumulative corrosion losses and the development of refined predictive formulas.

Based on the expanded dataset, the present study extends the previous descriptive assessment into a predictive modelling framework. The principal methodological advance is the reformulation of cumulative steel replacement as a ship–structural-area prediction problem, supported by renewal-based deterioration modelling, cell-level machine learning, ship-wise cross-validation, and stochastic uncertainty quantification. This structure allows information from a small but highly heterogeneous fleet sample to be used more efficiently, while preserving ship-level independence during validation and enabling prospective prediction for technically specified ships outside the historical sample. The main contributions of this research are as follows: (i) total amount of cumulative lifetime steel replaced is extracted from company reports for selected ships and hull lightweight groups, (ii) based on these data, a total amount of cumulative lifetime material wastage loss is calculated for ships, and (iii) a mathematical framework for the cumulative steel replacement is developed for similar ships (main contribution). Thus, this study addresses the main question: can cumulative steel replacement be predicted for a ship whose technical characteristics are known, even when the ship itself is not part of the historical sample used for model development? The paper answers this question through two complementary model families. The first family is a renewal-based parametric framework for cumulative steel replacement and maintenance scheduling. The second family is a cell-level machine-learning framework for steel replacement prediction. For both model families, deterministic and stochastic variants were implemented.

2. Materials

The data used in this study were extracted from reports provided by a certified thickness measurement company (see Acknowledgements), approved by IACS classification societies. The company conducted ultrasonic thickness measurements throughout the service lives of the ships. The available records covered 71 bulk carriers and were initially screened to identify vessels exhibiting more pronounced corrosion degradation

and substantial cumulative steel replacement. Based on this initial screening, 12 Handymax bulk carriers were selected for detailed data extraction and analysis. For these ships, the underlying thickness-measurement and steel-renewal records were subsequently examined and systematically processed at both ship and structural-area levels. Four of the selected vessels had already been analysed in our earlier study [56], while eight additional ships were included in the present work. The purpose of this selection was not to obtain a statistically representative sample of the overall Handymax bulk-carrier population, but to investigate cumulative steel replacement in severely corrosion-affected vessels. Consequently, the analysed dataset should be regarded as a deliberately restricted, corrosion-intensive subset of the available database. The predictive models developed in this study are therefore intended primarily for ships with technical characteristics and degradation severity comparable to those represented in the present sample. Application to vessels experiencing low or moderate corrosion degradation requires additional validation. Within the extracted series of bulk carriers, 7 were carrying iron, ore and coal (Table 1), and 5 were carrying grain (Table 2). Original data for 4 bulk carriers (labelled as S_1, S_2, S_3 and S_4, in Table 1) were presented in [56]. Steel replaced (*SR*) is expressed in tons as a cumulative value standardised to a 25-year-equivalent service horizon. This does not imply that all ships were decommissioned or observed for exactly 25 years, but that the data were transformed into a common temporal basis for comparison and prediction. All ships were in Handymax range of deadweight (selected ships: 38110-48826 t dwt), as defined by Clarkson in [53] and given a class by IACS classification societies. Their lengths vary between 173 m and 199 m.

Table 1 Bulk carriers carrying iron, ore and coal

Ship label	S_1	S_2	S_3	S_4	S_5	S_6	S_7
Length overall, L_{OA} [m]	199	199	197.6	187	187	183	180
Breadth, B [m]	29	29	28.3	28.4	28	31	31
Year built, YB	1982	1982	1983	1983	1978	1984	1984
Class	BV	BV	LR	LR	BV	DNV	ABS
Gross tonnage, GT [/]	25056	25056	25742	22112	22372	24844	17599
Deadweight, DWT [t]	44504	44504	41427	38110	38972	42312	42390
Cargo group	Iron/ore/coal	Iron/ore/coal	Iron/ore/coal	Iron/ore/coal	Iron/ore/coal	Iron/ore/coal	Iron/ore/coal
Total steel replacement, SR_S [t] (25-year equivalent)	1292	1472	873	443	828	1072	596

Table 2 Bulk carriers carrying grain

Ship label	S_8	S_9	S_{10}	S_{11}	S_{12}
Length overall, L_{OA} [m]	179	175	173	173	173
Breadth, B [m]	27	26	26	26	26
Year built, YB	1984	1982	1984	1984	1980
Class	BV	BV	BV	BV	LR
Gross tonnage, GT [/]	19045	17436	15220	15200	16591
Deadweight, DWT [t]	48826	47871	41920	41920	42617
Cargo group	grain	grain	grain	grain	grain
Total steel replacement, SR_S [t] (25-year equivalent)	331	21	183	175	25

Additionally, cumulative 25-year steel replacement data were extracted from reports for 11 structural areas (i.e., lightweight mass groups). The raw data on steel replacements are provided in Appendix A, which also includes minimum thickness reduction criteria used for steel replacement and records of corrosion wastage observed. These groups encompass all structural elements subject to corrosion monitoring and steel replacement, as required by the classification society for each ship. The structure includes plating and internal

components such as girders, webs, transverses, stiffeners, and brackets (see Table 3 for a detailed explanation of the lightweight groups).

Table 3 Structural areas (lightweight groups)

Lightweight group label (acronym)	Lightweight group full name	Structure included	Loads
1. UD	Upper deck	From aft end to fore end of ships. Plates included; no stiffeners included.	Exposed to conditions within ballast tanks and cargo holds, as well as to the outdoor atmosphere from the upper side of the deck.
2. DS	Deck superstructure	Aft part of ships, above upper deck. Plates included; no internal structure included.	Exposed to the outdoor atmosphere, while the lower deck structure is generally insulated and located in a closed atmospheric environment.
3. BSSP	Bottom and side shell platings	From aft end to fore end of ships. Plates included; no internal structure included.	Exposed to the atmosphere and seawater from the outside, as well as to the influences of ballast, cargo, and dry or wet air from the inside.
4. HCC	Hatch cover and coaming	Along the length of cargo holds. Plates and internal structure included.	Exposed to atmospheric conditions.
5. ISTST	Internal structure in top side tanks	Along the length of cargo holds. Internal structure included.	Exposed to ballast water or dry and humid air within the tank, and to atmospheric conditions from the outside (lateral and upper surfaces). Depending on the conditions inside the cargo holds, the tanks may also be influenced by either the ambient atmosphere or the nature of the cargo loaded.
6. CHTB	Cargo holds transverse bulkheads	In cargo holds. Flat bulkheads with stiffeners or corrugated bulkheads included.	Exposed to cargo influences or, when empty, to atmospheric conditions inside the hold. Bulkheads between holds are affected on both sides, with cargo handling having a particularly strong impact in this region.
7. CHMF	Cargo holds main frames (with brackets)	In cargo holds. Main frames with brackets included.	Exposed to the medium, cargo, and enclosed atmospheric conditions within the holds, as well as to the effects of cargo handling practices.
8. IBHP	Inner bottom and hopper platings	Along the length of cargo holds. Plates included.	Exposed to cargo or atmospheric conditions within the cargo holds, and to the effects of handling equipment from above. From below, the steel plates are subjected to conditions within ballast tanks (i.e., ballast water and enclosed dry or humid air), fuel in fuel tanks, and dry internal atmospheric conditions.
9. ISDBT	Internal structure in double bottom tanks	Along cargo holds. Internal structure.	Exposed to fuel, ballast, and dry or humid air may be present inside the tanks; while seawater, cargo, and atmospheric conditions (in empty cargo holds) act from the outside.
10. APS	Aft peak tank	Aft end of ships. Plates and internal structure included; outer shell is not included.	Exposed internally to media such as technical or drinking water, ballast water, or dry and humid air. The outer side, i.e., shell plating, is subjected to seawater, atmospheric conditions, and closed or semi-closed ambient environments.
11. FPS	Fore peak tank	Fore end of ships. Plates and internal structure included; outer shell is not included.	Exposed internally to media such as technical or drinking water, ballast water, or dry and humid air. The outer side, i.e., shell plating, is subjected to seawater, atmospheric conditions, and closed or semi-closed ambient environments.

For a reference bulk-carrier design maintained at one of the shipyards, the original steel mass of each structural area was available as a percentage of the ship deadweight. The area-share coefficient is denoted by $w_a = LWT_a^{ref}/DWT^{ref}$, where LWT_a^{ref} is the original steel mass of area a and DWT^{ref} is the deadweight

of the reference ship. Table 4 reports $100w_a$ in percent; consequently, the tabulated percentages are divided by 100 before w_a is used in Equation (1). These data were originally presented in [56]. The reference "similar" ship has the following principal particulars: 29,850 GT, 52,000 dwt, 189.9 m length overall, and 32.24 m breadth. These data are used to estimate the original weights of the lightweight groups.

Table 4 The amount of steel in tons and in relation to deadweight in each of 11 lightships subgroups - obtained for a "similar" bulk carrier - from [56]

Structural area, a	$100\mathrm{w_a} = 100\,\mathrm{LWT_a^{ref}}/DWT^{ref}$ [%]
1. UD	0.81
2. DS	0.88
3. BSSP	2.99
4. HCC	1.35
5. ISTST	1.57
6. CHTB	1.20
7. CHMF	0.55
8. IBHP	1.62
9. ISDBT	2.68
10. APS	0.42
11. FPS	0.69

3. Methods

The analysis was performed on a ship dataset (Table 1 and 2) in which each ship was described by its technical characteristics and each structural area was represented by a relative share of ship deadweight mass (Table 4). For each ship s and structural area a (i.e., each of the $N_A = 11$ lightweight groups), the steel mass (1) represented by that area (i.e., lightweight group) is defined as:

$$M_{a,s} = w_a DWT_s \tag{1}$$

where $M_{a,s}$ is the modelled steel mass in area a of the ship s measured in tons, w_a is the dimensionless area-share coefficient defined from the reference ship in Table 4, and DWT_s is the deadweight tonnage of the ship s measured in tons. The threshold mass (2) associated with replacement is then:

$$H_{a,s} = \theta_{a,s} M_{a,s} \tag{2}$$

where $H_{a,s}$ is the threshold mass in tons and $\theta_{a,s}$ is the threshold fraction, which is unitless. The observed replaced fraction (3) is defined as:

$$F_{a,s}^{obs} = \frac{SR_{a,s}^{obs}}{M_{a,s}} \tag{3}$$

where $F_{a,s}^{obs}$ is a unitless ratio and $SR_{a,s}^{obs}$ is the non-standardised observed replaced steel mass in tons.

Equation (4) allow us to compare the observed replacement directly with the threshold mass:

$$Q_{a,s}^{obs} = \frac{SR_{a,s}^{obs}}{H_{a,s}} \tag{4}$$

where $Q_{a,s}^{obs}$ is unitless.

Because the available observation horizon was not identical for all ships, the cumulative observed replacement was normalized to a common 25-year-equivalent scale:

$$SR_{a,s} = SR_{a,s}^{obs} \frac{25}{T_s} \tag{5}$$

where $SR_{a,s}$ is the cumulative steel replacement in area a of ship s, expressed in tons and normalised to a 25-year-equivalent horizon, and T_s is the actual observation horizon of ship s in years. In the present dataset, eleven of the twelve ships already correspond to a 25-year observation horizon. Only ship S11 was observed over 30 years and therefore required temporal standardization and its cumulative replacement values were multiplied by 25/30. This transformation is used solely to place the observed response on a common exposure-equivalent scale for model training and should not be interpreted as a linear corrosion or renewal law. The temporal evolution of deterioration and the discrete nature of renewal events are represented separately in the renewal-based modelling framework. From this point onward, $\mathrm{SR}_{a,s}$ and its ship-level aggregate $\mathrm{SR_s}$ denote the 25-year-equivalent quantities; the superscript obs is retained only for non-standardised observations. For the ship-level presentations in Figures 1 and 6 and Tables 1 and 2, $\mathrm{SR_s} = \sum_{a=1}^{N_A} SR_{a,s}$, whereas Figures 2 and 7 and Appendix A retain the structural-area level, using $\mathrm{SR}_{a,s}$.

The renewal-based parametric framework models deterioration and replacement on an inspection grid. In its deterministic form, it provides a central renewal-based estimate, while in its stochastic form it provides simulated replacement trajectories and predictive intervals. Time was discretized on an inspection grid with a constant step of $\Delta = 2.5$ years. In all deterministic and stochastic renewal simulations, the corrosion-initiation delay was fixed at $T_{init} = 10$ years. The parameter T_{init} is distinct from the inspection-grid interval Δ. Following a replacement event, the age of the renewed element is reset to zero, and the same initiation delay is applied before active deterioration resumes. The active corrosion age (6) is defined as:

$$A_{a,s}(t) = \max(0, t - T_{init}) \tag{6}$$

where $A_{a,s}(t)$ is the active corrosion age in years for area a of ship s at time t, and T_{init} is corrosion-initiation delay measured in years. Under a linear loss law, the fractional loss is written as:

$$L_{a,s}^{lin}(t) = r_{a,s} A_{a,s}(t) \tag{7}$$

where $L_{a,s}^{lin}(t)$ is the unitless fractional loss and $r_{a,s}$ is the linear deterioration rate measured in inverse years. Equation (7) assumes proportional deterioration growth after corrosion initiation.

Under a nonlinear loss law, the deterioration is expressed as:

$$L_{a,s}^{nonlin}(t) = k_{a,s} A_{a,s}(t)^{\beta} \tag{8}$$

where $L_{a,s}^{nonlin}(t)$ is the unitless nonlinear loss, $k_{a,s}$ is the scale parameter, and β is the shape parameter controlling acceleration. Equation (8) allows deterioration to intensify nonlinearly with time.

In the replacement criterion, $L_{a,s}(t)$ denotes the deterioration law selected for the considered model, i.e., either $L_{a,s}^{\mathrm{lin}}(t)$ or $L_{a,s}^{\mathrm{nonlin}}(t)$. Replacement is triggered (9) when the local loss reaches or exceeds the threshold fraction:

$$I_{a,s}(t) = \begin{cases} 1, & L_{a,s}(t) \geq \theta_{a,s} \\ 0, & L_{a,s}(t) < \theta_{a,s} \end{cases} \tag{9}$$

where $I_{a,s}(t)$ is a binary replacement indicator.

For any requested horizon X, the deterministic cumulative replacement in one area is then:

$$C_{a,s}(X) = \sum_{k=1}^{K} R_{a,s}(t_k)\, \mathbf{1}(t_k \leq X) \tag{10}$$

where $C_{a,s}(X)$ is the cumulative replaced steel mass in area a of ship s up to horizon X; $R_{a,s}(t_k)$ is the steel mass replaced at inspection time t_k; K is the total number of inspection points considered; and $\mathbf{1}(t_k \leq X)$ is an indicator equal to 1 when the inspection time does not exceed the requested horizon. Equation (10) therefore accumulates all renewal events up to X.

The total ship-level cumulative replacement (11) is obtained by aggregation over structural areas:

$$C_s(X) = \sum_{a=1}^{N_A} C_{a,s}(X) \tag{11}$$

where $C_s(X)$ is the cumulative replacement of ship s at horizon X measured in tons.

A one-at-a-time sensitivity analysis was performed to assess the dependence of the renewal-based predictions on the principal modelling assumptions. Starting from the baseline specification, the inspection-grid interval, deterioration-initiation delay T_{init}, deterioration law, and replacement-threshold regime were varied separately while all other model components were held fixed. The inspection interval was evaluated at 1.25, 2.5, and 5 years, and T_{init} at 5, 10, and 15 years. Both the linear and nonlinear deterioration laws were considered. Threshold sensitivity was evaluated by multiplying the baseline threshold values by factors of 0.8, 1.0, and 1.2; for area-specific threshold regimes, the same multiplier was applied to each area-specific value. For each scenario, cumulative replacement at the 25-year horizon was recalculated and expressed both in tons and as a relative change from the baseline prediction. The sensitivity analysis evaluates the numerical robustness of the renewal-based predictions without altering or refitting the machine-learning component.

The cell-level machine-learning framework uses each ship-area combination as a separate predictive observation. Its target is the 25-year-equivalent replaced fraction:

$$F_{a,s} = \frac{SR_{a,s}}{M_{a,s}} \tag{12}$$

where $F_{a,s}$ is a unitless target variable. Equation (12) is important because it shifts the prediction problem from absolute tons to a scale-adjusted fraction.

Three deterministic point-estimate predictors were evaluated: Gradient Boosting Regressor (GBR), Ridge regression, and GBR with an additional log-total correction step. The fitted model f relates the cell-level predictor vector $\mathbf{x}_{a,s}$ to the target defined in Equation (12):

$$\hat{F}_{a,s} = f(\mathbf{x}_{a,s}). \tag{13}$$

where $\hat{F}_{a,s}$ is the predicted replaced fraction. It is converted back to tons and aggregated to ship level as:

$$\widehat{SR}_{a,s} = \hat{F}_{a,s} M_{a,s}, \qquad \widehat{SR}_s = \sum_{a=1}^{N_A} \widehat{SR}_{a,s}. \tag{14}$$

where $\widehat{\mathrm{SR}}_{a,s}$ is the predicted 25-year-equivalent steel replacement in area a of ship s and $\widehat{\mathrm{SR}}_s$ is the corresponding predicted ship-level total, both expressed in tons.

Deterministic predictive performance of the cell-level machine-learning models was assessed by leave-one-ship-out cross-validation (LOOCV). In each split, all rows belonging to one ship were removed from the training set, the candidate model was fitted on the remaining ships, and prediction was generated for the held-out ship. This protocol was chosen because the practical deployment question is not interpolation within the same ship, but generalization to a ship whose historical replacement profile is unknown. Model selection was based primarily on ship-level root-mean-square error (RMSE) and mean absolute error (MAE), and the final point-estimate model was selected from the compared GBR, GBR with log-total correction, and Ridge regression alternatives.

To characterise the uncertainty of the aggregate LOOCV error estimates, the ship-level out-of-fold prediction errors were additionally resampled with replacement. For each bootstrap replicate, RMSE and MAE were recalculated from the resampled set of 12 held-out ship errors, and the 2.5th and 97.5th percentiles were used to obtain empirical 95 % intervals. Because the LOOCV training sets overlap substantially, these intervals are interpreted as descriptive measures of validation-error variability rather than as formal confidence intervals based on independent test samples.

The stochastic layer belongs to the renewal-based framework and is used to express uncertainty explicitly. The stochastic renewal-based framework uses Monte Carlo simulation to generate repeated cumulative replacement trajectories under uncertain deterioration rates and threshold-triggered replacement events. For a given ship and horizon, the mean cumulative replacement over stochastic realizations (15) is:

$$\overline{C}_s(X) = \frac{1}{J}\sum_{j=1}^{J} C_s^{(j)}(X) \tag{15}$$

where $\overline{C}_s(X)$ is the mean cumulative replacement in tons and $C_s^{(j)}(X)$ is the cumulative replacement from Monte Carlo realization j. The predictive interval (16) is then defined through empirical quantiles:

$$PI_s^{lo}(X) = Q_{\alpha/2}\left(C_s^{(1)}(X), \ldots, C_s^{(J)}(X)\right), \qquad PI_s^{hi}(X) = Q_{1-\alpha/2}\left(C_s^{(1)}(X), \ldots, C_s^{(J)}(X)\right) \tag{16}$$

where $PI_s^{lo}(X)$ and $PI_s^{hi}(X)$ are the lower and upper predictive limits in tons, $Q_{\alpha/2}$ and $Q_{1-\alpha/2}$ are the empirical lower and upper quantiles of the simulated cumulative replacements and α is the nominal tail probability. The same mean and quantile definitions are applied at structural-area level by replacing $C_s^{(j)}(X)$ with $C_{a,s}^{(j)}(X)$, yielding $\overline{C}_{a,s}(X)$, $\mathrm{PI}_{a,s}^{\mathrm{lo}}(X)$, and $\mathrm{PI}_{a,s}^{\mathrm{hi}}(X)$.

In addition to the validation performed on the observed ships, the workflow includes a prospective inference protocol for a technically specified ship that is not part of the observed sample. This prospective application is intended to demonstrate model deployment and should not be interpreted as independent validation in the absence of observed steel-replacement data for that ship. The input vector of the new ship is written as:

$$\mathbf{z}^{\mathrm{new}} = [\mathrm{cargo}, \mathrm{class}, DWT^{\mathrm{new}}, LOA^{\mathrm{new}}, B^{\mathrm{new}}, GT^{\mathrm{new}}, YB^{\mathrm{new}}, X, \theta\text{-mode}] \tag{17}$$

where DWT^{new} is deadweight in tons, LOA^{new} is length overall in metres, B^{new} is breadth in metres, GT^{new} is gross tonnage, YB^{new} is year built, X is the requested prediction horizon in years, and θ-mode denotes the threshold regime, and it can be fixed for some usual value for all ship areas, or each area can have its specific value. The prospective demonstration ship was transformed into the same eleven-area structural representation as the observed fleet.

For the prospective demonstration ship, M_a^{new} and H_a^{new} are calculated analogously to Equations (1) and (2). Its deterministic renewal-based total at horizon X is denoted by $C^{\mathrm{new}}(X)$, following Equation (11), while the stochastic mean and predictive limits are denoted by $\overline{C}^{\mathrm{new}}(X)$, $\mathrm{PI}_{\mathrm{new}}^{\mathrm{lo}}(X)$, and $\mathrm{PI}_{\mathrm{new}}^{\mathrm{hi}}(X)$, following Equations (15) and (16).

4. Results and discussions

The cumulative steel replacement (SR) standardized to a 25-year-equivalent service period exhibits considerable variability among the investigated bulk carriers. Within the analysed dataset, a clear difference can be observed between ships carrying grain and those transporting iron ore and coal. In general, the investigated vessels operating in the iron/ore/coal trade exhibited substantially higher cumulative steel renewal than the grain carriers. This observation should, however, be interpreted as an association within the present sample rather than as a direct causal effect of cargo type, since other vessel-specific and operational factors may also contribute to the observed differences. Furthermore, the distribution of steel replacement among structural regions is highly non-uniform. In particular, the inner bottom and hopper plating (IBHP) accounts for approximately 47.6 % of the total 25-year-equivalent steel replacement recorded across the 12 analysed ships, indicating that nearly one half of the cumulative renewal demand is concentrated in this structural region, see Appendix A. From an engineering perspective, this pronounced concentration is relevant for structural-area-specific inspection, thickness monitoring, corrosion-protection measures, and steel-renewal planning. It also identifies the IBHP region as deserving particular attention in life-cycle structural assessment, although the present dataset alone is not sufficient to prescribe changes to design corrosion margins.

Quantitatively, the 25-year-equivalent cumulative steel replacement ranges from 21 to 1472 t across the 12 analysed ships, with a mean of 609.3 t, a standard deviation of 495.9 t, and a coefficient of variation of 81.4 %. The variability is partly structured by cargo group: iron/ore/coal ships show a mean of 939.4 t and a coefficient of variation of 39.0 %, whereas grain ships show a mean of 147.0 t and a coefficient of variation of 87.8 %. These values confirm substantial heterogeneity within the analysed corrosion-intensive fleet and

reinforce the need to interpret predictions within the empirical domain represented by the sample rather than as population-wide estimates.

Figure 1 presents the cumulative steel replacements (SR_s) extracted from the database for all considered ships as a function of ship length and cargo type (grain or iron ore/coal). A clear positive correlation between ship length and cumulative steel replacement can be observed. Within the analysed fleet, larger ships generally required greater amounts of steel replacement throughout their service life, with the increase being approximately proportional to ship length. In addition, the cumulative steel replacements and minimum thickness reduction criteria for steel replacements ($\theta_{a,s}$) are given for each of $N_A = 11$ lightweight groups ($SR_{a,s}$) and for the ship under consideration (SR_s), see Figure 2. The data exhibit considerable scatter, preventing the identification of a distinct trend or relationship.

In Figure 3, the steel mass of the lightweight groups ($M_{a,s}$) and of the ship under consideration (M_s) is estimated using Equation (1) and the data presented in Table 4. Consequently, the corresponding threshold masses of the lightweight groups ($H_{a,s}$) and of the ship (H_s), representing the minimum estimated masses after corrosion-induced wastage during service, were determined using Equation (2) and are presented in Figure 4. Likewise, Equation (3) was used to determine the fraction of replaced steel relative to the lightweight group mass ($F_{a,s}$) and to the total ship steel mass (F_s), as shown in Figure 5. The four data points from these diagrams corresponding to the original ships listed in Tables 1 and 2 have previously been published in [56]. Although some relationships exhibit approximately linear behaviour while others show considerable scatter, the primary purpose of Figures 3-5 is to present the processed dataset that forms the basis for the mathematical framework developed in Section 3. The results obtained using this methodology are presented and discussed in the following section.

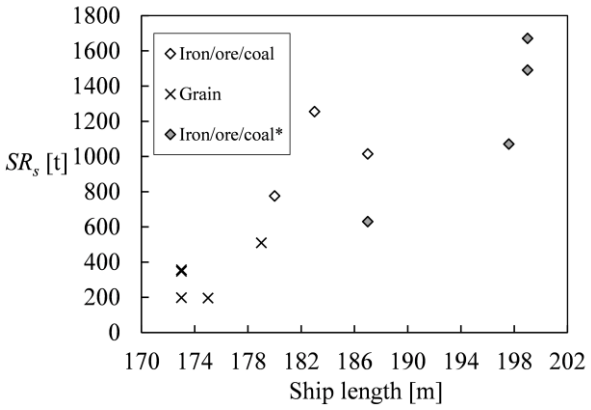


Fig. 1 Ship-level cumulative steel replacement SR_s, expressed on a 25-year-equivalent basis (* denotes data published in [56])

The predictive models were evaluated using the assumptions and validation procedures defined in Section 3. The deterministic cell-level models were assessed as point-estimate predictors, while the stochastic renewal-based framework was used to represent replacement schedules and predictive uncertainty.

The deterministic validation results and stochastic diagnostic summaries are shown together in Table 5. The deterministic cell-level point-estimate models were evaluated using leave-one-ship-out cross-validation. Among these models, the cell-level GBR model achieved the lowest RMSE and MAE. The renewal-based and stochastic outputs were evaluated separately as diagnostic and schedule-based summaries. Therefore, their RMSE and MAE values should be interpreted as observed-fleet diagnostic errors rather than as directly comparable LOOCV validation errors. The term hybrid refers to the combination of the renewal-based deterioration-and-replacement mechanism with empirical ship-level and area-level calibration terms, introduced to improve agreement with the observed replacement data.

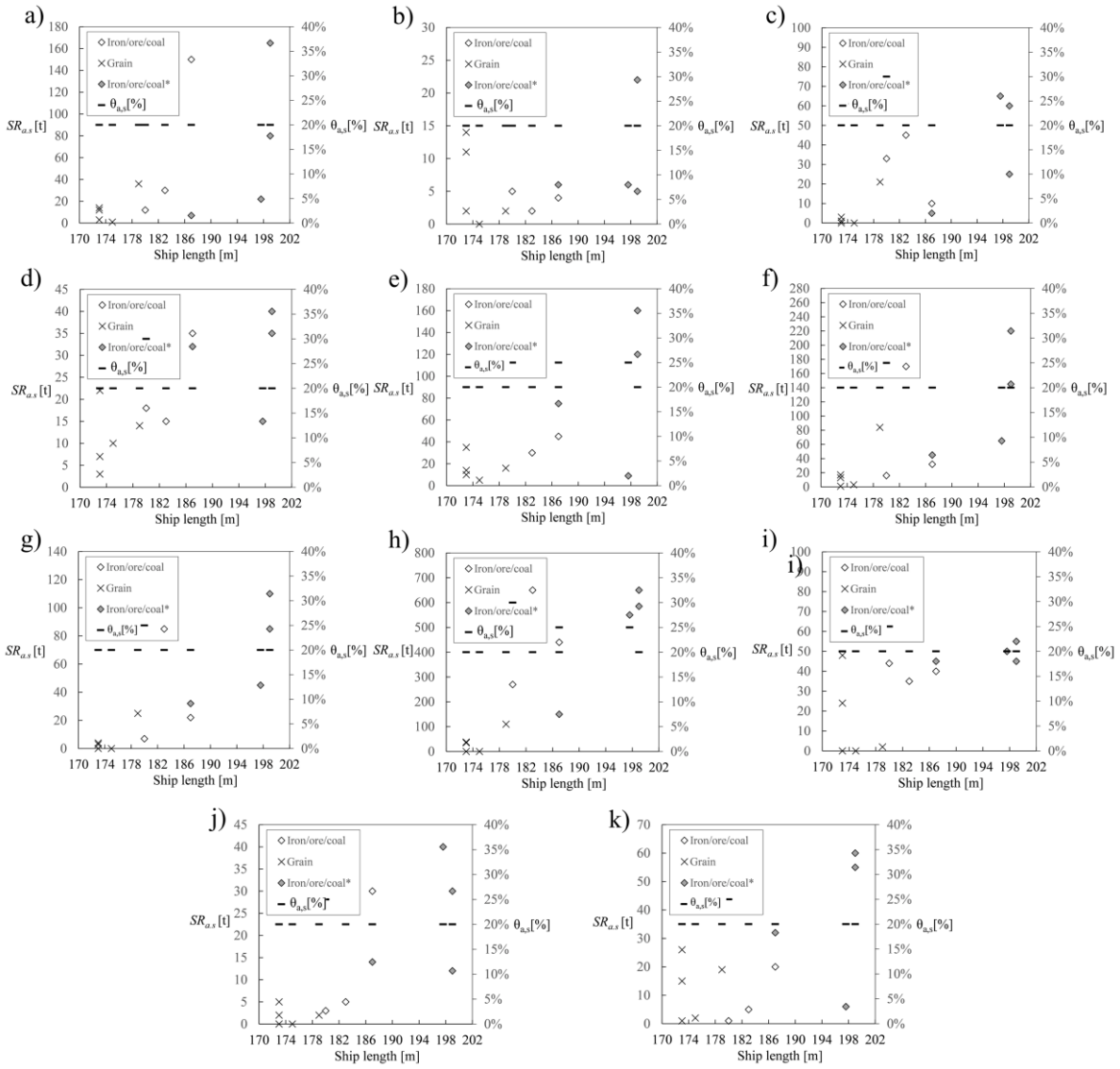


Fig. 2 Cumulative steel replacements ($SR_{a,s}$) and minimum thickness reduction criteria for steel replacements ($\theta_{a,s}$) by a lightweight group (* denotes data published in [56]): a) 1. UD, b) 2. DS, c) 3. BSSP, d) 4. HCC, e) 5. ISTST, f) 6. CHTB g) 7. CHMF, h) 8. IBHP, i) 9. ISDBT, j) 10. APS, k) 11. FPS

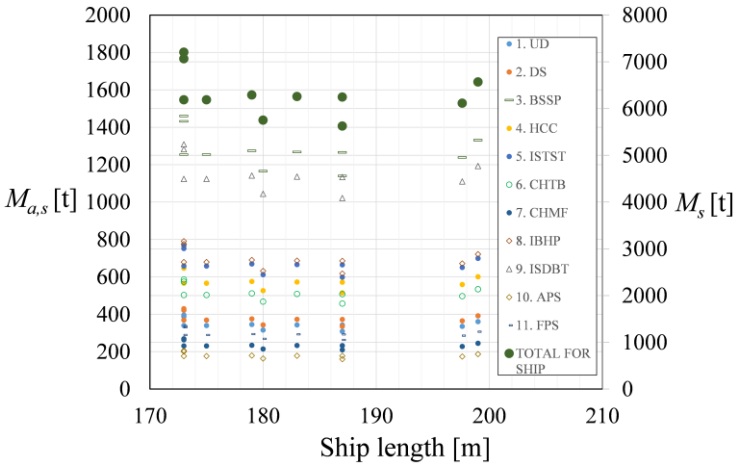


Fig. 3 Steel mass of the lightweight groups ($M_{a,s}$) and the steel mass of ship under consideration (M_s)

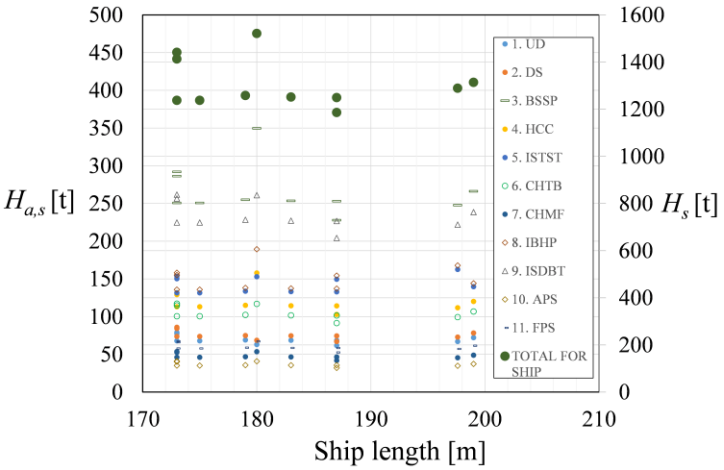


Fig. 4 Threshold mass of the lightweight groups ($H_{a,s}$) and the the ship under consideration (H_s)

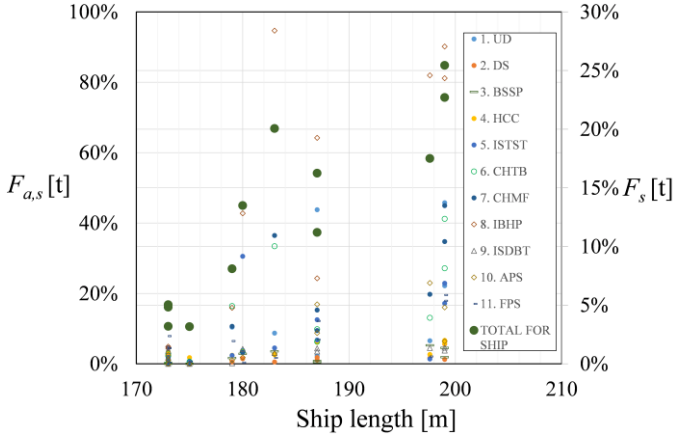


Fig. 5 Share (fraction) between the replaced steel mass and the mass for the lightweight groups ($F_{a,s}$) and the same share on the level of a whole ship (F_s)

Table 5 Deterministic validation results and stochastic diagnostic summaries

Deterministic point-estimate models	RMSE [t]	MAE [t]	Observed-fleet fitted and stochastic diagnostic summaries	Type	RMSE [t]	MAE [t]
Cell-level GBR	227.78	178.87	Renewal-based hybrid point estimate	fitted diagnostic summary	239.45	182.59
Cell-level GBR + logTotalCorr	236.48	180.23	Cell-level machine-learning point estimate	in-sample fitted diagnostic summary	38.00	22.61
Cell-level Ridge	430.51	275.66	Schedule mean	Monte Carlo schedule summary	581.92	495.93

Note: The left part of the table reports leave-one-ship-out cross-validation errors for deterministic cell-level point-estimate models. The right part reports observed-fleet diagnostic summaries, including renewal-based and stochastic schedule outputs. These values are useful for comparing fitted and schedule-based behaviour, but they should not be interpreted as directly equivalent to the LOOCV errors reported for the deterministic point-estimate models.

As a robustness check, the leave-one-ship-out analysis was repeated without applying the 25-year standardization to S11. The selected GBR model remained unchanged, while ship-level RMSE changed by approximately 2 % and MAE by less than 1 %. Thus, the normalization of the single 30-year observation did not materially affect model selection or predictive performance. The uncertainty of these aggregate LOOCV metrics was also examined across the 12 held-out ships. For the selected cell-level GBR model, the absolute ship-level errors had a standard deviation of 147.30 t, a median of 143.23 t, and an interquartile range of 81.40-223.78 t. Ship-level bootstrap resampling of the out-of-fold errors yielded empirical 95 % intervals of 104.77-262.99 t for MAE and 130.77-305.95 t for RMSE. These relatively broad intervals reflect the limited number

of independent ships and indicate that the reported validation metrics should be interpreted as sample-specific performance estimates rather than precise population-level quantities.

A separate sensitivity analysis of the renewal-based model assumptions showed that the renewal-based predictions were most strongly affected by the deterioration-initiation delay. Relative to the baseline $T_{\text{init}} = 10$ years, reducing T_{init} to 5 years increased the median 25-year cumulative replacement across the analysed ships by 75.6 %, whereas increasing it to 15 years reduced it by 66.0 %. Threshold perturbations produced smaller but still substantial effects, with median changes of +28.1 % and −20.0 % for 0.8 and 1.2 times the baseline thresholds, respectively. Substitution of the baseline nonlinear deterioration law by the correspondingly calibrated linear formulation resulted in a median change of 7.7 %. Variations in the inspection-grid interval from 2.5 years to 1.25 or 5 years did not change the cumulative 25-year replacement total in the analysed cases, although the coarser 5-year grid delayed the median first predicted replacement from 12.5 to 15.0 years.

Figure 6 compares the observed ship-level cumulative replacement totals with the main fitted and renewal-based summaries. The cell-level machine-learning point estimate follows the observed totals closely in the fitted diagnostic comparison, while the renewal-based hybrid estimate and the stochastic schedule mean show larger deviations for several ships. This figure should therefore be interpreted as a diagnostic comparison within the analysed dataset, whereas the LOOCV results in Table 5 provide the validation-based assessment of deterministic point-estimate performance.

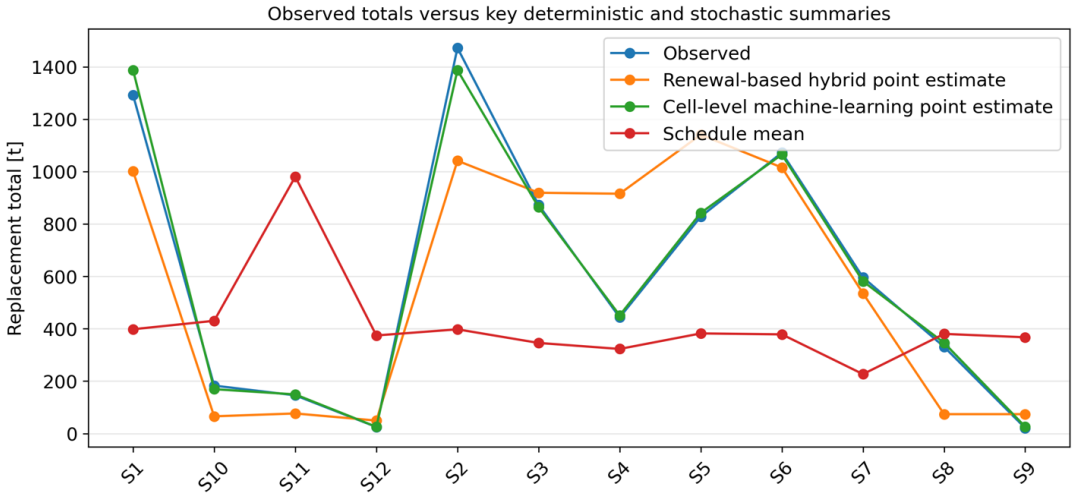
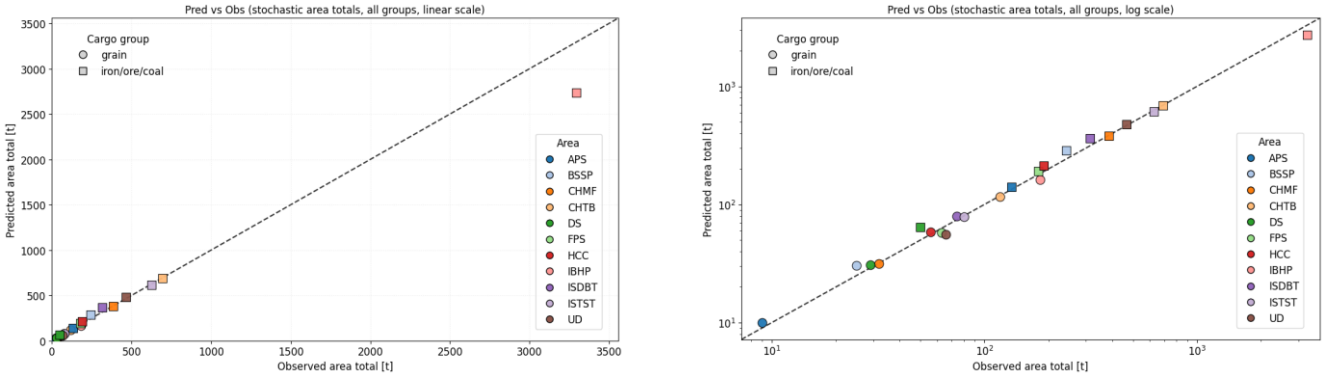


Fig. 6 Observed-fleet prediction overview across main approaches

A diagnostic comparison between observed and predicted steel replacement was also performed at the level of structural areas, as shown in Figure 7.



a) b)

Fig. 7 Observed versus predicted area-level steel replacement totals for grain and iron/ore/coal ships: a) linear scale; b) logarithmic scale

Figure 7 compares the observed and predicted 25-year-equivalent steel replacement totals for the two cargo groups, grain and iron/ore/coal. The colours indicate structural areas, while the marker shapes distinguish the cargo groups. The dashed diagonal represents perfect agreement between observed and predicted values. Figure 7a presents the results on the original linear scale, allowing the absolute magnitude of prediction deviations to be assessed directly in tons. Figure 7b presents the same data on logarithmic axes, which improves the visibility of structural areas with substantially smaller replacement totals. The two representations are therefore complementary: the linear scale emphasizes absolute prediction error, whereas the logarithmic scale facilitates comparison across the full range of observed replacement magnitudes.

The predictive performance reported above is based on ship-wise leave-one-ship-out validation. The following new-ship case is presented as a prospective application of the calibrated framework and should not be interpreted as independent external validation, because no observed steel-replacement outcome is available for this generated ship. The selected cell-level machine-learning point-estimate model was then applied prospectively to a technically specified demonstration ship, NEW_GRAIN_01, whose input characteristics are presented in Table 6. The purpose of this example is to illustrate inference for a ship outside the observed sample rather than to provide independent validation, since no measured steel-replacement outcome is available for this case. The stochastic renewal-based framework was subsequently used to obtain the replacement schedule and predictive intervals for the same ship.

Table 6 Input specification for the prospective demonstration ship

ship_name	cargo	class	DWT^{new} [t]	LOA^{new} [m]	B^{new} [m]	GT^{new} [/]
NEW_GRAIN_01	grain	BV	42617.0	173.0	26.0	16591.0

The specification of NEW_GRAIN_01 follows Equation (17) and is summarised in Table 6. Cargo group and class are categorical descriptors, whereas DWT^{new}, LOA^{new}, B^{new}, GT^{new}, and YB^{new} describe the ship geometry and age. The requested horizon is $X = 20$ years. For the grain-cargo example, θ-mode is fixed at $\theta_a^{\mathrm{new}} = 0.20$ for all structural areas, in accordance with the calibration results for this cargo group. For iron/ore/coal ships, area-specific threshold values provided better agreement and should therefore be used instead of the fixed regime. The tail probability is $\alpha = 0.05$, corresponding to a constructed 95 % predictive interval.

For NEW_GRAIN_01, the total stochastic steel replacement was estimated by Monte Carlo simulation. Table 7 reports the quantities defined in Equations (15) and (16) using $J = 300$ realisations. The stochastic mean $\overline{C}^{\mathrm{new}}(20) = 55.84$ t, while $\mathrm{PI}^{\mathrm{lo}}_{\mathrm{new}}(20) = 43.68$ t and $\mathrm{PI}^{\mathrm{hi}}_{\mathrm{new}}(20) = 68.21$ t were obtained as empirical quantiles for $\alpha = 0.05$. The selected deterioration law was nonlinear, as defined in Equation (8), with parameters calibrated from the observed ship dataset for the relevant cargo group and threshold regime.

Table 7 Stochastic total replacement at the requested horizon

ship	cargo	X [years]	$\overline{C}^{\mathrm{new}}(X)$ [t]	$\mathrm{PI}^{\mathrm{lo}}_{\mathrm{new}}(X)$ [t]	$\mathrm{PI}^{\mathrm{hi}}_{\mathrm{new}}(X)$ [t]
NEW_GRAIN_01	grain	20.0	55.84	43.68	68.21

Table 8 is not obtained by proportionally splitting the ship-level total. Each structural-area quantity is produced directly by the same stochastic renewal simulation. The table reports $\overline{C}_a^{\mathrm{new}}(X)$, $\mathrm{PI}^{\mathrm{lo}}_{a,\mathrm{new}}(X)$, and $\mathrm{PI}^{\mathrm{hi}}_{a,\mathrm{new}}(X)$, using the area-level extension of Equations (15) and (16). Equation (11) is then used to aggregate the area-level stochastic means to the ship-level value reported in Table 7. The sum of $\overline{C}_a^{\mathrm{new}}(20)$ over all structural areas is 55.84 t, consistent with $\overline{C}^{\mathrm{new}}(20)$.

Table 8 Stochastic area-level replacement at the requested horizon for NEW_GRAIN_01

Area, a	θ_a^{new} [-]	M_a^{new} [t]	$\overline{C}_a^{\text{new}}(X)$ [t]	$\text{PI}_{a,\text{new}}^{\text{lo}}(X)$ [t]	$\text{PI}_{a,\text{new}}^{\text{hi}}(X)$ [t]
IBHP	0.2	690.395	33.901	24.164	44.013
CHTB	0.2	511.404	9.642	5.418	14.064
FPS	0.2	294.057	5.338	2.941	8.454
UD	0.2	345.198	3.399	1.294	6.267
ISTST	0.2	669.087	2.138	0.000	5.018
CHMF	0.2	234.394	0.573	0.000	1.465
HCC	0.2	575.330	0.489	0.000	1.438
DS	0.2	375.030	0.322	0.000	1.406
ISDBT	0.2	1142.136	0.033	0.000	1.000
APS	0.2	178.991	0.005	0.000	0.000
BSSP	0.2	1274.248	0.003	0.000	0.000

Figure 8a shows the stochastic cumulative schedule for the NEW_GRAIN_01 ship, i.e., the cumulative replacement of steel over time, up to the selected horizon of 20 years. In that panel, the solid line represents the mean cumulative replacement over time, while the shaded band represents the predictive interval. The values are shown at discrete inspection points, i.e., every 2.5 years.

Figure 8b shows the contribution of each structural area to the cumulative replacement at the selected horizon. The bar height represents the stochastic mean $\overline{C}_a^{\text{new}}(20)$, while the error bars indicate the corresponding predictive interval from $\text{PI}_{a,\text{new}}^{\text{lo}}(20)$ to $\text{PI}_{a,\text{new}}^{\text{hi}}(20)$.

5. Conclusions

The results of the conducted analysis show that cumulative steel replacement can be estimated based on ship characteristics and information at the level of structural areas, i.e., ship lightweight groups. The best leave-one-ship-out predictive performance was achieved by the deterministic cell-level GBR point-estimate model. In addition, the stochastic renewal-based formulation provided schedule-based outputs, predictive intervals, and insight into the temporal evolution and structural-area distribution of cumulative steel replacement.

The workflow was also applied prospectively to a demonstration ship whose technical characteristics remained within the range represented by the analysed fleet. This application demonstrates prospective use of the framework within the observed empirical domain and does not constitute independent external validation, since no observed steel-replacement outcome is available for direct comparison. For such a ship, the deterministic point-estimate model can estimate cumulative steel replacement at a specified service horizon, while the stochastic renewal-based framework provides replacement schedules, area-level decomposition, and predictive intervals. Independent validation on additional ships with measured steel-replacement histories would be required to assess the broader predictive generalizability of the framework.

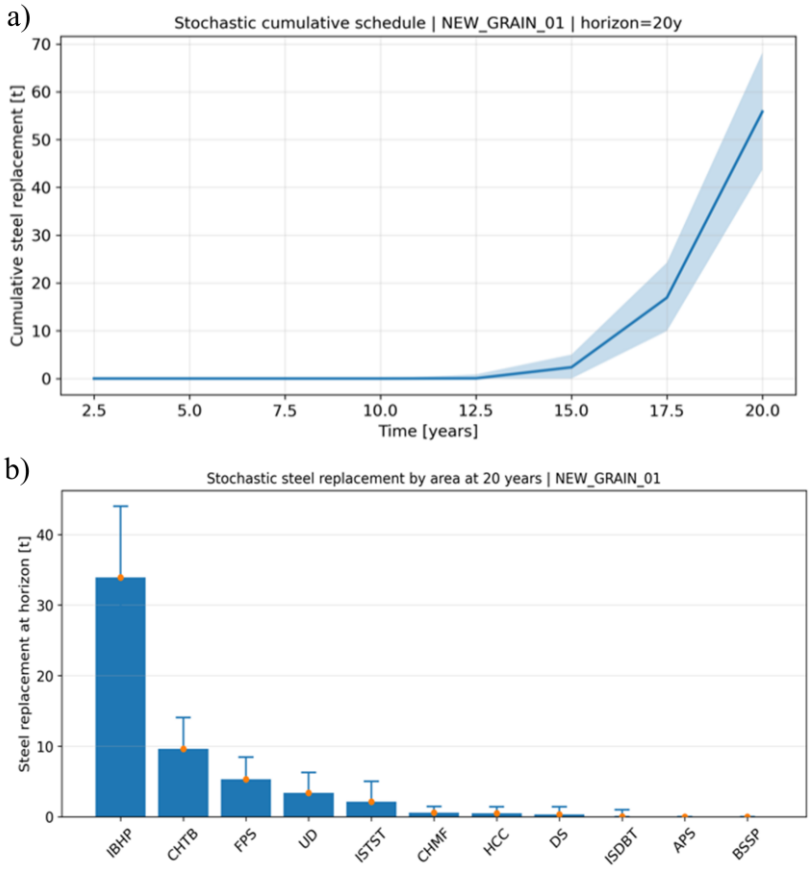


Fig. 8 Stochastic generated ship outputs: a) stochastic cumulative schedule with predictive interval; b) stochastic area-level replacement with predictive intervals

From an engineering perspective, the results demonstrate that cumulative steel replacement over a typical 25-year service life can exceed 1000 t in severely corrosion-affected Handymax bulk carriers, highlighting the significant maintenance demands associated with long-term corrosion. Steel renewal was found to be highly non-uniformly distributed among structural areas, with the inner bottom and hopper plating accounting for approximately 47.6 % of the total 25-year-equivalent replacement recorded across the analysed ships. This concentration of renewal demand has practical implications for structural-area-specific inspection and maintenance planning, particularly for prioritizing thickness monitoring, corrosion protection and steel renewal in the most affected regions. Furthermore, within the analysed sample, ships carrying iron ore and coal generally exhibited substantially greater steel renewal than grain carriers. This difference should not be attributed to cargo type alone, since other factors such as vessel characteristics, coating condition, maintenance history, trading pattern, classification requirements, and loading/unloading practices may also contribute to long-term structural deterioration.

The results presented in this study should be interpreted within the limits of the analysed dataset. Since the investigated vessels represent a corrosion-intensive subset of Handymax bulk carriers, the proposed prediction framework is presently applicable only within a comparable range of ship particulars and degradation severity. Broader application to the general Handymax population or to vessels with less pronounced corrosion degradation would require further validation using additional data.

The presented methodology also enables estimation of cumulative corrosion-induced material loss and lightweight group masses, providing information relevant for maintenance planning, ship design, structural assessment, and life-cycle management of aging vessels. In addition, the quantified amounts of replaced steel contribute to understanding the material flows associated with ship maintenance and recycling.

ACKNOWLEDGMENTS

This research is supported by the approved thickness measurement company - INVAR-Ivošević Company. More information about the company can be found at URL: http://www.invar.me/index.html. The data are collected and systematized during the lifetime of ships by the company operators and experts, and thus, used here for the analysis.

APPENDIX A

Table A1 Data on cumulative steel replacement ($SR_{a,s}$ and SR_s), minimum thickness reduction criteria for steel replacements ($\theta_{a,s}$) and corrosion wastage recorded in the 25th year of service after cumulative 25-year period steel is already replaced (Corr25), for 11 lightweight groups and ships: S_1-S_4

Ship label	S_1			S_2			S_3			S_4		
Ship region	$SR_{a,s}$ [t]	$\theta_{a,s}$ [%]	Corr25 [%]	$SR_{a,s}$ [t]	$\theta_{a,s}$ [%]	Corr25 [%]	$SR_{a,s}$ [t]	$\theta_{a,s}$ [%]	Corr25 [%]	$SR_{a,s}$ [t]	$\theta_{a,s}$ [%]	Corr25 [%]
1. UD	10	20	10 – 15	165	20	10 – 15	22	20	5 – 10	7	20	5 – 10
2. DS	5	20	10 – 15	22	20	5 – 10	6	20	5 – 10	6	20	5 – 10
3. BSSP	25	20	0 – 5	60	20	0 – 5	65	20	0 – 5	5	20	0 - 5
4. HCC	35	20	5 – 10	40	20	5 – 10	15	20	0 – 5	32	20	0 – 5
5. ISTST	120	20	5 – 10	160	20	0 – 5	9	25	0 – 5	75	25	0 – 5
6. CHTB	220	20	5 – 10	145	20	0 – 5	65	20	0 – 5	45	20	0 – 5
7. CHMF	110	20	5 – 10	85	20	5 – 10	45	20	5 – 10	32	20	0 – 5
8. IBHP	585	20	5 – 10	650	20	5 – 10	550	25	5 – 10	150	25	0 – 5
9. ISDBT	45	20	0 – 5	55	20	5 – 10	50	20	5 – 10	45	20	0 – 5
10. APS	12	20	0 – 5	30	20	5 – 10	40	20	5 – 10	14	20	0 – 5
11. FPS	55	20	0 - 5	60	20	5 – 10	6	20	5 – 10	32	20	0 – 5
Total (SR_s)	1292			1472			873			443		

Table A2 Data on cumulative steel replacement ($SR_{a,s}$ and SR_s), minimum thickness reduction criteria for steel replacements ($\theta_{a,s}$) and corrosion wastage recorded in the 25th year of service after cumulative 25-year period steel is already replaced (Corr25), for 11 lightweight groups and ships: S_5-S_8

Ship label	S_1			S_2			S_3			S_4		
Ship region	$SR_{a,s}$ [t]	$\theta_{a,s}$ [%]	Corr25 [%]	$SR_{a,s}$ [t]	$\theta_{a,s}$ [%]	Corr25 [%]	$SR_{a,s}$ [t]	$\theta_{a,s}$ [%]	Corr25 [%]	$SR_{a,s}$ [t]	$\theta_{a,s}$ [%]	Corr25 [%]
1. UD	150	20	5 – 10	30	20	0 – 5	12	20	10 – 15	36	20	0 – 5
2. DS	4	20	5 – 10	2	20	0 – 5	5	20	0 – 5	2	20	0 – 5
3. BSSP	10	20	0 – 5	45	20	0 – 5	33	30	5 – 10	21	20	0 – 5
4. HCC	35	20	5 – 10	15	20	0 – 5	18	30	10 – 15	14	20	0 – 5
5. ISTST	45	20	0 – 5	30	20	0 – 5	187	25	5 – 10	16	20	0 – 5
6. CHTB	32	20	0 – 5	170	20	5 – 10	16	25	5 – 10	84	20	5 – 10
7. CHMF	22	20	0 – 5	85	20	5 – 10	7	25	0 – 5	25	20	5 – 10
8. IBHP	440	20	5 – 10	650	20	5 – 10	270	30	10 – 15	110	20	5 – 10
9. ISDBT	40	20	0 – 5	35	20	0 – 5	44	25	0 – 5	2	20	0 – 5
10. APS	30	20	0 – 5	5	20	0 – 5	3	25	0 – 5	2	20	0 – 5
11. FPS	20	20	0 – 5	5	20	0 – 5	1	25	0 - 5	19	20	0 – 5
Total (SR_s)	828			1072			596			331		

Table A3 Data on cumulative steel replacement ($SR_{a,s}$ and SR_s), minimum thickness reduction criteria for steel replacements ($\theta_{a,s}$) and corrosion wastage recorded in the 25th year of service after cumulative 25-year period steel is already replaced (Corr25), for 11 lightweight groups and ships: S_9-S_{12}

Ship label	S_9			S_{10}			S_{11}			S_{12}		
Ship region	$SR_{a,s}$ [t]	$\theta_{a,s}$ [%]	Corr25 [%]	$SR_{a,s}$ [t]	$\theta_{a,s}$ [%]	Corr25 [%]	$SR_{a,s}$ [t]	$\theta_{a,s}$ [%]	Corr25 [%]	$SR_{a,s}$ [t]	$\theta_{a,s}$ [%]	Corr25 [%]
1. UD	1	20	0 - 5	12	20	5 – 10	14	20	5 - 10	3	20	0 – 5
2. DS	0	20	0 – 5	14	20	10 – 15	11	20	5 – 10	2	20	0 – 5
3. BSSP	0	20	0 – 5	3	20	0 - 5	0	20	0 – 5	1	20	0 – 5
4. HCC	10	20	0 – 5	7	20	0 – 5	22	20	0 – 5	3	20	0 – 5
5. ISTST	5	20	0 – 5	14	20	0 – 5	35	20	0 – 5	10	20	0 – 5
6. CHTB	3	20	0 – 5	13	20	0 – 5	17	20	0 – 5	1	20	0 – 5
7. CHMF	0	20	0 – 5	3	20	5 – 10	0	20	0 – 5	4	20	0 – 5
8. IBHP	0	20	0 – 5	38	20	10 – 15	35	20	5 – 10	0	20	0 – 5
9. ISDBT	0	20	0 – 5	48	20	0 – 5	24	20	0 – 5	0	20	0 – 5
10. APS	0	20	0 – 5	5	20	0 – 5	2	20	0 – 5	0	20	0 – 5
11. FPS	2	20	0 – 5	26	20	0 – 5	15	20	0 – 5	1	20	0 – 5
Total (SR_s)	21			183			175			25		

REFERENCES

[1] Yamamoto, N., Kumano, A., Matoba, M., 1994. Effect of corrosion and its protection on hull strength (2nd Report). *Journal of the Society of Naval Architects of Japan*, 176, 281-289. https://doi.org/10.2534/jjasnaoe1968.1994.176_281

[2] Eyres, D. J., 2007. Ship construction. Sixth Edition. *Butterworth-Heinemann*. https://doi.org/10.1016/B978-075068070-7/50017-7

[3] Paik, J. K., Melchers, R. E., 2008. Condition assessment of aged structures. *CRC Press, Woodhead Publishing Limited*. https://doi.org/10.1533/9781845695217

[4] Viner, A. C., Tozer, D. R., 1985. Influence of corrosion on ship structural performance. Hull New Construction Division No. 85/29, *Lloyd's Register of Shipping*.

[5] Paik, J. K., Brennan, F., Carlsen, C. A., Daley, C., Garbatov, Y., Ivanov, L., Rizzo, C., Simonsen, B. C., Yamamoto, N., Zhuang, H. Z., 2006. Report of Committee V.6: Condition Assessment of Aging Ships. *16th International Ship and Offshore Structures Congress*, 20-25 August, Southampton, UK.

[6] Roberts, S. E., Marlow, P. B., 2002. Casualties in dry bulk shipping (1963-1996). *Marine Policy*, 26, 437-450. https://doi.org/10.1016/S0308-597X(02)00024-6

[7] International Maritime Organization, IMO, 2007. Bulk carrier casualty report. MSC 83/INF.6, 3 July 2007. *International Maritime Organization*, London, UK.

[8] Heij, C., Knapp, S., 2019. Shipping inspections, detentions, and incidents: an empirical analysis of risk dimensions. *Maritime Policy & Management*, 46(7), 866-883. https://doi.org/10.1080/03088839.2019.1647362

[9] Barbulescu, A., Dumitriu, C. S., 2023. Fractal characterization of brass corrosion in cavitation field in seawater. *Sustainability*, 15, 3816. https://doi.org/10.3390/su15043816

[10] Yamamoto, N., Ikegami, K., 1996. A study on the degradation of coating and corrosion of ship's hull based on the probabilistic approach. *International Offshore Mechanics and Arctic Engineering Symposium* (OMAE'96), 16-21 June, Florence, Italy, 2, 159-166.

[11] Kovač, N., Ivošević, Š., Momčilović, N., 2024. Corrosion-induced thickness diminution of an ageing bulk carrier. *Brodogradnja*, 75(4), 75404. https://doi.org/10.21278/brod75404

[12] Rodkina, A., Ivanova, O., Kramar, V., Dushko, V., Zhilenkov, A., Chernyi, S., Zinchenko, A., 2022. Simulation and selection of protection types in the design stage of ships and offshore structures. *Brodogradnja*, 73(2), 59-77. https://doi.org/10.21278/brod73204

[13] Guedes Soares, C., Garbatov, Y., 1999. Reliability of maintained, corrosion protected plates subjected to non-linear corrosion and compressive loads. *Marine Structures*, 12(6), 425-445. https://doi.org/10.1016/S0951-8339(99)00028-3

[14] Melchers, R. E., 1999. Corrosion uncertainty modelling for steel structures. *Journal of Constructional Steel Research*, 52(1), 3-19. https://doi.org/10.1016/S0143-974X(99)00010-3

[15] Melchers, R. E., 2003. Probabilistic model for marine corrosion of steel for structural reliability assessment. *Journal of Structural Engineering*, 129(11), 1484-1493. https://doi.org/10.1061/(ASCE)0733-9445(2003)129:11(1484)

[16] Abbas, M., Rizvi, S. H. M., Sarfraz, S., Raza, A., Khan, A., Loya, A., Najib, A., 2024. Evaluation of the influence of dissolved nitrates on corrosion behaviour of ship structural steel exposed to seawater environment. *Ocean Engineering*, 298. https://doi.org/10.1016/j.oceaneng.2024.117268

[17] Ozturk, M. C., Coghlan, L., Zimina, M., Akid, R., Martin, T. L., Larrosa, N. O., 2025. Corrosion behaviour of 316L stainless steel under stress in artificial seawater droplet exposure at elevated temperature and humidity. *Corrosion Science*, 254. https://doi.org/10.1016/j.corsci.2025.113039

[18] Vukelić, G., Vizentin, G., Brnić, J., Brčić, M., Sedmak, F., 2021. Long-term marine environment exposure effect on butt-welded shipbuilding steel. *Journal of Marine Science and Engineering*, 9. https://doi.org/10.3390/jmse9050491

[19] Vukelić, G., Mihaljec, B., Ivošević, Š., 2025. Marine environment effect on welded additively manufactured stainless steel AISI 316L. *Journal of Marine Science and Engineering*, 13 https://doi.org/10.3390/jmse13030459

[20] Paik, J. K., Thayamballi, A. K., Park, Y. I., Hwang, J. S., 2004. A time-dependent corrosion wastage model for seawater ballast tank structures of ships. *Corrosion Science*, 46(2). https://doi.org/10.1016/S0010-938X(03)00145-8

[21] Guedes Soares, C., Garbatov, Y., Zayed, A., Wang, G., 2008. Corrosion wastage model for ship crude oil tanks. *Corrosion Science*, 50(11). https://doi.org/10.1016/j.corsci.2008.08.035

[22] Ivošević, Š., Meštrović, R., Kovač, N., 2019. Probabilistic estimates of corrosion rate of fuel tank structures of aging bulk carriers. *International Journal of Naval Architecture and Ocean Engineering*, 11(1), 165-177. https://doi.org/10.1016/j.ijnaoe.2018.03.003

[23] Ivošević, Š., Kovač, N., Momčilović, N., Vukelić, G., 2021. Analysis of corrosion depth percentage on the inner bottom plates of aging bulk carriers with an aim to optimize corrosion margin. *Brodogradnja*, 72(3), 72306. https://doi.org/10.21278/brod72306

[24] Ohyagi, M., 1987. Statistical survey on wear of ships' structural members. *Nippon Kaiji Kyokai Technical Bulletin*, 5.

[25] Paik, J. K., Kim, S. K., Lee, S. K., 1998. A probabilistic corrosion rate estimation model for longitudinal strength members of bulk carriers. *Ocean Engineering*, 25(10), 837-860. https://doi.org/10.1016/S0029-8018(97)10009-9

[26] Ivošević, Š., Kovač, N., Momčilović, N., Vukelić, G., 2022. Evaluation of the corrosion depth of double bottom longitudinal girder on aging bulk carriers. *Journal of Marine Science and Engineering*, 10(10). https://doi.org/10.3390/jmse10101425

[27] Paik, J. K., Thayamballi, A. K., 2002. Ultimate strength of aging ships. *Journal of Engineering for the Maritime Environment*, 1(1), 57-77. https://doi.org/10.1243/147509002320382149

[28] Paik, J. K., Lee, J. M., Park, Y. I., Hwang, J. S., Kim, C. W., 2003. Time-variant ultimate longitudinal strength of corroded bulk carriers. *Marine Structures*, 16, 567-600. https://doi.org/10.1016/j.marstruc.2004.01.003

[29] Momčilović, N., Ilić, N., Kalajdžić, M., Ivošević, Š., Petrović, A., 2023. Pitting and uniform corrosion effects on ultimate strength of a bulk carrier. *Procedia Structural Integrity*, 48. https://doi.org/10.1016/j.prostr.2023.07.104

[30] Momčilović, N., Ilić, N., Kalajdžić, M., Ivošević, Š., Petrović, A., 2024. Effect of corrosion-induced structural degradation on the ultimate strength of a high-tensile-steel ship hull. *Journal of Marine Science and Engineering*, 12. https://doi.org/10.3390/jmse12050745

[31] Woloszyk, K., Goerlandt, F., Montewka, J., 2024. A methodology for ultimate strength assessment of ship hull girder accounting for enhanced corrosion degradation modelling. *Marine Structures*, 93. https://doi.org/10.1016/j.marstruc.2023.103530

[32] Wang, Y., Wharton, J. A., Shenoi, R. A., 2014. Ultimate strength analysis of aged steel-plated structures exposed to marine corrosion damage: a review. *Corrosion Science*, 86. https://doi.org/10.1016/j.corsci.2014.04.043

[33] Tekgoz, M., Garbatov, Y., Guedes Soares, C., 2020. Review of ultimate strength assessment of ageing and damaged ship structures. *Journal of Marine Science and Application*, 19. https://doi.org/10.1007/s11804-020-00179-7

[34] Det Norske Veritas, DNV, 2016. Rules for Classification of Ships. *Det Norske Veritas*, Oslo, Norway.

[35] Bureau Veritas, BV, 2025. Rules for the classification of steel ships. *Bureau Veritas*, Paris, France.

[36] Lloyd's Register, LR, 2020. Rules and regulations for the classification of ships. *Lloyd's Register*, London, UK.

[37] International Association of Classification Societies, IACS, 2024. Common Structural Rules for Bulk Carriers and Oil Tankers. *International Association of Classification Societies*, London, UK.

[38] Poggi, L., Gaggero, T., Gaiotti, M., Ravina, E., Rizzo, C., 2020. Recent developments in remote inspections of ship structures. *International Journal of Naval Architecture and Ocean Engineering*, 12, 881-891. https://doi.org/10.1016/j.ijnaoe.2020.09.001

[39] American Bureau of Shipping, ABS, 2025. Rules for Building and Classing Marine Vessels. *American Bureau of Shipping*, USA.

[40] Watson, D. G. M., 1998. Practical ship design. *Elsevier Science Ltd.*, Oxford, UK.

[41] Schneekluth, H., Bertram, V., 1998. Ship design for efficiency and economy. Second Edition. *Butterworth-Heinemann*, Oxford, UK.

[42] Papanikolaou, A., 2014. Ship design: methodologies of preliminary design. *Springer*, Dordrecht, Netherlands. https://doi.org/10.1007/978-94-017-8751-2

[43] Inal, O. B., 2024. Decarbonization of shipping: hydrogen and fuel cells legislation in the maritime industry. *Brodogradnja*, 75(2), 75205. https://doi.org/10.21278/brod75205

[44] Prados, J. M., Fernandez, I. A., Gomez, M. R., Parga, M. N., 2024. The decarbonisation of the maritime sector: Horizon 2050. *Brodogradnja*, 75(2), 75202. https://doi.org/10.21278/brod75202

[45] Grlj, C., Degiuli, N., Martić, I., 2025. Scale effects on the resistance and propulsion characteristics of the Japan Bulk Carrier. *Ocean Engineering*, 339, Part 1. https://doi.org/10.1016/j.oceaneng.2025.122059

[46] International Maritime Organization, IMO, 2018. Resolution MEPC.308(73). Guidelines on the method of calculation of the attained Energy Efficiency Design Index (EEDI) for new ships. *International Maritime Organization*, London, UK.

[47] International Maritime Organization, IMO, 2021. Resolution MEPC.328(76). *International Maritime Organization*, London, UK.

[48] International Maritime Organization, IMO, 2006. Application of SOLAS regulation XII/6.3 on corrosion prevention of dedicated seawater ballast tanks in all types of ships and double-side skin spaces of bulk carriers and application of the performance standard for protective coatings for dedicated seawater ballast tanks in all types of ships and double-side skin spaces of bulk carriers. *International Maritime Organization*, London, UK.

[49] International Maritime Organization, IMO, 2010. Resolution MSC.289(87). *International Maritime Organization*, London, UK.

[50] International Maritime Organization, IMO, 2012. Annex 4 - Resolution MEPC.210(63). Adopted on 2 March 2012 - 2012 Guidelines for safe and environmentally sound ship recycling. *International Maritime Organization*, London, UK.

[51] International Maritime Organization, IMO, 2017. Linkages between IMO's technical assistance work and the 2030 Agenda for Sustainable Development. *International Maritime Organization*, London, UK.

[52] UN Trade and Development, UNCTAD, 2024. Review of Maritime Transport. *UN Trade and Development*.

[53] Clarkson, 2025. Bulk vessel sizes - a guide to bulk vessel sizes. https://www.clarksons.com/glossary/a-guide-to-bulk-vessel-sizes/ (accessed 26 August 2025)

[54] Kalajdžić, M., Vasilev, M., Momčilović, N., 2022. Power reduction considerations for bulk carriers with respect to novel energy efficiency regulations. *Brodogradnja*, 73(2), 73205. https://doi.org/10.21278/brod73205

[55] Vasilev, M., Kalajdžić, M., 2022. Influence of lightweight change on ship performance. *FME Transactions*, 50(4). https://doi.org/10.5937/fme2204615V

[56] Momčilović, N., Ivošević, Š., Kovač, N., 2025. Lifetime corrosion loss of bulk carriers. *TransNav - International Journal on Marine Navigation and Safety of Sea Transportation*, 19. https://doi.org/10.12716/1001.19.01.28

[57] Gratsos, G. A., Psaraftis, H. N., Zachariadis, P., 2009. Life cycle cost of maintaining the effectiveness of a ship's structure and environmental impact of ship design parameters: an update. *RINA Conference on the Design and Operation of Bulk Carriers*, 26-27 October, Athens, Greece.